ELSEVIER

Coordination Chemistry Reviews
211 (2001) 25–43

COORDINATION CHEMISTRY REVIEWS

www.elsevier.com/locate/ccr

Intermediates in chromium(III) photochemistry

Garth Irwin, Alexander D. Kirk *

Department of Chemistry, University of Victoria, PO Box 3065, Victoria, BC, Canada, V8W 3V6

Received 14 June 1999; accepted 10 January 2000

Contents

Abstract

A review of proposed intermediates and transition states for Cr(III) photosubstitution processes shows that several competing ideas have been presented. A survey of the available experimental evidence reveals, however, only one instance of a well characterized intermedi-

* Corresponding author. Tel.: +1-250-7217173; fax: +1-250-7217147.
E-mail address: smtp.kirk@phys.uvic.ca (A.D. Kirk).

PII: S0010-8545(00)00281-2

ate with measurable lifetime, that for *cis*-Cr(cyclam)$(NH_3)_2^{3+}$. Study of this and other hexam(m)ine Cr(III) complexes by laser flash photolysis with conductivity detection found other examples of transient conductivity increases associated with intermediate chemistry but confirms that the *cis*-Cr(cyclam)$(NH_3)_2^{3+}$ intermediate is so far unique in having a low-pH conductivity decay lifetime longer than that of its parent's doublet state. The behavior of the complexes has been modeled via numerical integration of the differential equations for the proposed kinetics after laser excitation, and the unique nature of *cis*-Cr(cyclam)$(NH_3)_2^{3+}$ is attributed to initial loss of a cyclam ring N atom with subsequent recombination and displacement of an ammonia ligand, consistent with the predictions of the angular overlap model of Cr(III) photosubstitution. The analysis indicates that about 30% of the reaction occurs directly from the quartet state, and that the ring-N mode constitutes about two-thirds of the photochemistry. For all the systems studied, the observed 'intermediates' were assigned as metastable six-coordinate primary photoproducts.

Keywords: Chromium(III); Photochemistry; Transition state

1. Background and introduction

This symposium is a testimony to the influence that Arthur Adamson has had on the development of inorganic photochemistry, not to mention surface chemistry, and on studies of photoprocesses in Cr(III) complexes in particular. Quite apart from his own major contributions, his ideas and proposals have been responsible for stimulating a great deal of research by others; the senior author of this paper wishes to acknowledge the great debt of gratitude owing to Adamson both for such stimulation of ideas and for Adamson's advice and assistance in his first efforts to contribute to the field of inorganic photochemistry. One of Adamson's major early contributions was the photochemical rules for Cr(III) complexes [1], which led directly to work confirming that his rule, loss of the strong field ligand on the weak field axis, was a useful special case of the broader explanation of Cr(III) photochemistry that subsequently developed [2,3] and which included the finding that stereochemical change was commonly associated with Cr(III) photosubstitution [2,3] and may even be a requirement [4,5] of the process. Along with the early efforts to rationalize the rules and their exceptions using MO calculations, this lead to the development of an angular overlap model for Cr(III) photochemistry [6] that gave a good rationale not only for the photolysis reaction modes but also for the stereochemical change associated with the light-induced chemistry.

The role of the doublet and quartet states in photochemistry has been a long standing problem since the earliest days of Cr(III) photochemistry and here we wish to avoid becoming embroiled in it. Current evidence is discussed [7] in a recent review. Most of the complexes of concern show two component photochemistry with the $\sim 25\%$ prompt and $\sim 75\%$ slow components giving essentially the same products and apparently occurring via a common pathway, most probably a quartet state species as proposed in Adamson's 1967 paper [1]. The angular overlap

model also starts with the assumption [8] that the photochemistry of Cr(III) complexes occurs from the quartet excited state; it is then considered to proceed with loss of the ligand with the weakest excited state bond strength, giving a five-coordinate intermediate with trigonal-bipyramidal (tbp) geometry. Association of a ligand with this intermediate then occurs in a symmetry-restricted fashion [9] such that the entering ligand occupies a position *cis* to the location vacated by the departed ligand, accounting for the stereochemical change. The intent of this contribution is to compare this model of the intermediates with a number of competing proposals that have appeared over the years and to examine the experimental evidence bearing on the question of intermediates in Cr(III) photochemistry.

For thermal reactions it is easy to distinguish a transition state, which exists at a maximum in potential energy along the reaction coordinate, from an intermediate which occurs at a local minimum. The distinctions are not always so clear with regard to photochemical processes, which are likely to be concerted, occurring by a cascade through states and configurations of progressively lower energy, possibly with no well defined maxima or minima. Since there is good evidence that Cr(III) photosubstitutions often take place on picosecond or sub-picosecond time scales, there is, at least in these instances, little room for significant activation barriers, and the distinction between intermediates and transition states loses much of its utility. This is reflected in the literature in that authors have tended to use the terms intermediate and transition state interchangeably. In what follows, we will continue to refer to intermediates, recognizing that the term transition state could be more appropriate in some cases given better knowledge of the energetics.

One of the first explorations of possible intermediates for thermal reactions of Cr(III) systems was included in the work of Spees, Perumareddi and Adamson [10]. They calculated the ligand field contributions to the stabilization energy for five- and seven-coordinate species of different coordination geometries and d orbital occupancy. They showed that for d^3 systems, the more likely intermediates were seven coordinate, but the energy contributions for pentagonal-bipyramidal and trapezoidal-octahedron (octahedral wedge) species were very similar and a choice could not be made. Unfortunately they did not extend their discussion to possible photochemical intermediates.

The discovery of the phenomenon of stereochemical change pointed to an associative, concerted mechanism for Cr(III) photosubstitution, but theoretical explorations at the time focussed only on the nature of labilization and the identity of the ligand preferentially labilized. Subsequently the advent of the angular overlap model provided [6,8,9] a reasonable explanation for both the ligand labilization and the stereochemical change inherent to the photochemistry, which was suggested to arise via symmetry restrictions on the formation and subsequent reactions of a five-coordinate tbp intermediate. Such an intermediate was inconsistent with volume of activation evidence [11–16] in favor of an associative pathway for Cr(III) photochemistry, and one of the authors has attempted to reconcile this by proposing [17] a pictorial representation of symmetry restricted associative interchange occurring via an asymmetric pentagonal-bipyramidal (apbp) intermediate. This

intermediate is obtained by attack of the entering ligand on an edge *trans* to the departing ligand as shown in Fig. 1(a).

A pentagonal-bipyramidal intermediate was also proposed [18] by others, while Wasgestian has suggested [19] an alternative pathway involving ligand loss followed by attack at an octahedral face *trans* to the departed ligand as shown in Fig. 1(b), giving a trigonal-prismatic six-coordinate intermediate which then collapses to the octahedral product. For these pathways the stereochemical outcomes are very similar and the differences between the two geometries would not be seen in the experiments that are feasible and have been done to date.

If, in Wasgestian's pathway, ligand entry precedes ligand loss, this gives a seven-coordinate face-capped trigonal prism, and this route was favored by Endicott [20]. However the angular overlap model [8,9,21] provides theoretical grounds to prefer the pathway via the apbp intermediate; the vacant t_{2g} orbital that invites nucleophilic attack by the entering ligand lies in the same plane as the leaving ligand, and interaction of the entering ligand with the cone of t_{2g}^2 electron density is avoided. These considerations suggest that the apbp route has the lowest

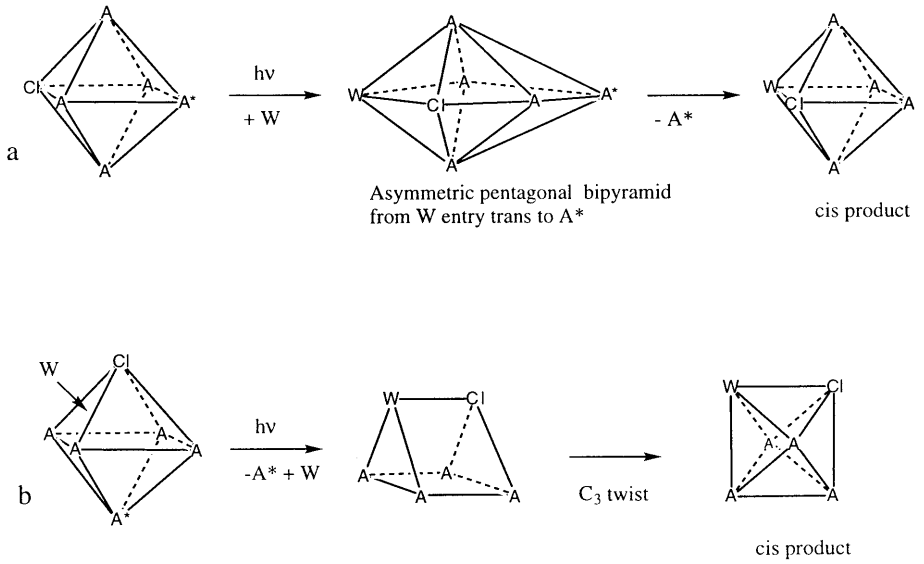

Fig. 1. Proposed intermediates or transition states for Cr(III) photosubstitution. (a) A seven-coordinate associative intermediate consistent with the angular overlap model [9]. Entry of a ligand W concerted with departure of the ligand A* from the lowest quartet excited state occurs via an asymmetric pentagonal-bipyramidal intermediate or transition state and leads to the cis product. This is consistent with the preferential labilization of the ligand A*, the availability of a vacant t_{2g} orbital which the entering Lewis base can attack, and the presence of a t_{2g}^2 cone of electron density either side of the pentagonal plane which inhibits out-of-plane ligand motions. (b) Wasgestian model[19]. Complete loss of the ligand A* followed by entry of W on a *trans* octahedral face leads to a six-coordinate trigonal-prismatic transition state that collapses via a trigonal twist to give the *cis* product.

electronic contributions to the energy barrier, and would be favored unless steric interactions dominate.

Turning now to the question of direct experimental evidence for any intermediates, this has been slow in coming. In studies of polypyridyl complexes, parallels between the thermal and photochemical behavior led to the suggestion that seven-coordinate intermediates were involved in the photochemistry [22–25], which for these complexes occurs almost exclusively via the doublet state. Experimental studies of the quartet state reactivity by study of the rate of product formation after a laser pulse have shown it to occur on the sub-nanosecond time scale, once more pioneering work by Adamson and co-workers [26]. The inference from studies of the rise-time of the doublet phosphorescence which is found to occur [27–30] on the picosecond or sub-picosecond time scale is more ambiguous. If the route of doublet population on quartet state excitation is intersystem crossing from the vibrationally relaxed quartet state, then the phosphorescence rise time truly indicates the time scale of equilibrated quartet reaction. However there is evidence that intersystem crossing may compete with vibrational relaxation, i.e. prompt intersystem crossing, and this then leaves room for a lifetime for the vibrationally relaxed quartet state in the picosecond to nanosecond domain. These rapid rates of reaction have rendered the search for intermediates difficult.

This situation changed when Waltz et al. reported [14,31] a microsecond intermediate present in the laser flash photolysis of *cis*-Cr(cyclam)$(NH_3)_2^{3+}$ monitored by the conductivity change in the solution. There were two important observations:

1. at a pH of 3.0 or below, a single exponential conductivity decrease was observed but with a lifetime that was more than twice the lifetime for the doublet phosphorescence under the same conditions;
2. at higher pH, a double exponential conductivity change was observed, corresponding first to a transient conductivity increase followed by an overall conductivity decrease, the extent of which showed a 'titration curve' corresponding to the pK_a of 4.0 of the final product, *cis*-Cr(cyclam)$(NH_3)(H_2O)^{3+}$.

These results were interpreted as showing that the reaction occurred, as shown in Fig. 2, via an aquo-intermediate, $I(OH_2)^{3+}$, with a pK_a of about 4.6, where the nature of this intermediate was unspecified. The authors recognized that it might be a seven-coordinate species, or it could be a six-coordinate species in which a water ligand had replaced a nitrogen of the cyclam ring. An important feature of the intermediate was its lifetime of 3.7 μs at room temperature.

The occurrence of this type of intermediate has remained unique to this complex to the present and it was of great interest to us to explore the generality of such intermediates and to obtain some clues as to the structure–reactivity criteria for their formation. We report here our confirmation of the behavior of *cis*-Cr(cyclam)$(NH_3)_2^{3+}$ and our studies of some other Cr(III) complexes using LFP with conductivity detection.

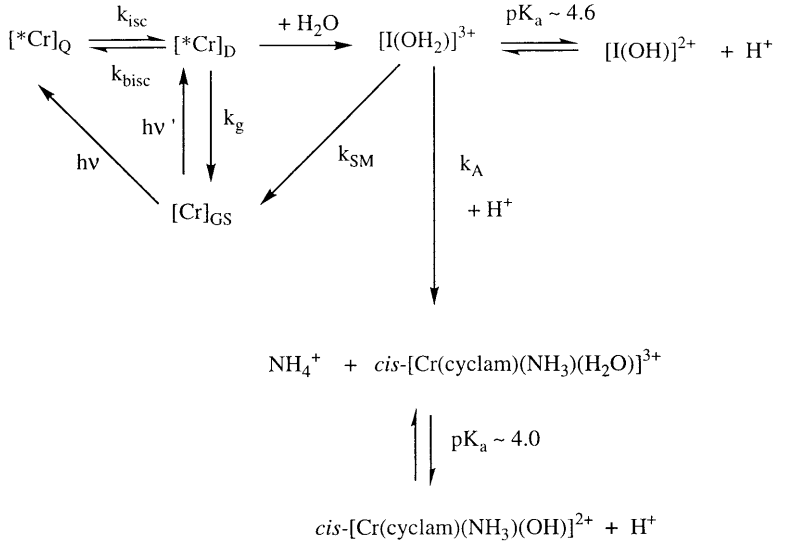

Fig. 2. Literature mechanism [14] for photosubstitution via a short-lived (microsecond) aquo-intermediate in *cis*-Cr(cyclam)$(NH_3)_2^{3+}$.

2. Experimental

2.1. Preparation of complexes

The complexes $[Cr(en)_3](ClO_4)_3$, $[Cr(tn)_3](ClO_4)_3$ and $[Cr(sen)](ClO_4)_3$ {sen = 4,4′4″-ethylidynetris(3-triazabutan-1-amine)} were available from previous studies [32–34]. The UV–vis spectra and emission lifetimes obtained for these complexes were compared to the literature values [32,33,35], confirming their purity.

$Cr(NH_3)_6^{3+}$ [36] and *cis*-Cr(cyclam)$(NH_3)_2^{3+}$ [37] were prepared following literature procedures and recrystallized as their perchlorate salts. Comparison of λ_{max}, ε_{max} and emission lifetimes with literature values confirmed the purity of these complexes.

trans-$Cr(tn)_2F_2^+$ was prepared by a modification [38] of the published method [39] for *trans*-$Cr(en)_2F_2^+$. The complex obtained was converted to the chloride salt of *trans*-$Cr(tn)_2(Cl)_2^+$ by overnight stirring in 38% HCl. Ammonolysis of the resulting *trans*-$[Cr(tn)_2(Cl)_2]Cl$ yielded a mixture of *cis*- and *trans*-$[Cr(tn)_2(NH_3)_2]Cl_3$. These isomers were separated as perchlorate salts by fractional recrystallization. Although the two isomers have identical λ_{max} values, they show small differences in ε_{max} and significantly different emission lifetimes. Lifetime and ε_{max} comparison with literature values [40] indicated the first batch of crystals obtained to be the *trans* isomer and the third batch to be the *cis* isomer.

2.2. Apparatus

The apparatus will be described in detail elsewhere [41]. Excitation was with a 5–10 ns pulse of ~40 mJ energy at 355 nm from the third harmonic of a Spectrophysics Nd/YAG laser, the 6 mm diameter beam passing between the upper two electrodes of the conductivity cell. This quartz-windowed cell, of path length 0.88 cm, has three platinum electrodes forming two compartments, connected such that the solution in the upper and lower compartments, respectively, form the sample and reference resistors for two arms of a Wheatstone bridge circuit that provides the input to a variable gain fast operational amplifier. When excited by a 120 V DC pulse of about 5 ms duration with the laser triggered on the flattest portion, this provides a transient conductivity signal to the Tektronix TDS 520 oscilloscope of the laser flash photolysis system. When signal averaging several transients, it was found advantageous to apply a second DC pulse of reverse polarity about 8 ms after the experiment pulse as this helped to reduce electrolysis and bubble formation at the electrodes. Signal acquisition is via a LABVIEW program written by Luis Netter of this department and data analysis makes use of the fitting routines provided by IGOR PRO 3.0(Wavemetrics).

2.3. Procedure

Measurements were made on fresh solutions circulated by a peristaltic pump at rates in the range 10–40 ml min^{-1} and this could be accomplished under a nitrogen atmosphere when desired. It was found to be crucial to use Viton tubing or stainless steel for all connections as other plastic tubings were found to leach plasticizers which generated interfering conductivity signals. Typical experimental conditions involved perchloric acid solutions, pH 2.6–5.1, which were approximately 1 mM in complex. The pH was measured using an Acumet 910 pH meter, with an Ingold Lot glass electrode. Data collection for each individual solution involved 3–5 repeat measurements, each consisting of 5–10 signal averaged shots. As the solution reservoir was large, relative to the volume irradiated, the continual flowing of solution ensured that secondary photolysis effects were minimal; the overall extent of photolysis rarely exceeded 2%. UV–vis spectra taken before and after photolysis confirmed that minimal changes in solution composition had occurred. Temperature within the laser laboratory is maintained at 20°C and the solutions were given adequate time to equilibrate to room temperature before data acquisition.

2.4. Emission lifetime measurements

Emission decay lifetime measurements were made on a different apparatus that excites samples using a PTA nitrogen laser delivering a pulse of about 1 mJ at 337 nm, duration of about 7 ns. Emission was monitored using a Jarrel–Ash monochromator/Hamamatsu GaAs photomultiplier. Lifetimes were evaluated from the slope of a weighted least-squares logarithmic plot of the data over 1024 points.

2.5. Data evaluation and curve fitting

All evaluations of experimental data and curve fitting of conductivity traces were carried out using IGOR PRO 3.0 (Wavemetrics, Inc) and the associated fitting procedures. The exponential and biexponential fitting procedures are iterative with the calculated chi-square values for each iteration being minimized using the Levenberg–Marquardt algorithm.

Simple modifications to the IGOR fitting procedures were made for calculation of the fraction of doublet photoreactions from conductivity traces displaying a biexponential decay. One program involved fitting the latter two thirds of these traces with an exponential fit and extrapolating to the onset of the laser pulse. The fraction of doublet photoreactions was then calculated from the ratio of the extrapolated decay to the overall experimental change in conductivity. An alternative method involved fitting the whole experimental trace to a double exponential fit. The fraction of doublet photoreactions was then calculated from the pre-exponential factors obtained by the fitting procedure, $F_D = A_1/(A_1 + A_2)$. A_1 and A_2 represent the pre-exponential factors for the slow and prompt components, respectively. In general, the two methods gave concordant F_D values.

3. Results

Several simple am(m)ine complexes of Cr(III) have been studied previously [42–45] by laser flash photolysis with conductivity detection at pH 3 or below but only for *cis*-Cr(cyclam)$(NH_3)_2^{3+}$ [14,31], Cr(bpy)$_3^{3+}$ [43], and Cr(phen)$_3^{3+}$ [45] has the pH dependence of the behavior been reported in detail. For those complexes that have been examined previously, Cr$(NH_3)_6^{3+}$, Cr(en)$_3^{3+}$, Cr(tn)$_3^{3+}$ at pH 3 or below, and for *cis*-Cr(cyclam)$(NH_3)_2^{3+}$ over the pH range 3–5, our results are in excellent agreement with the published data.

3.1. Emission and conductivity lifetimes

Emission lifetimes were measured at 20°C for the complexes in the study and the results are compared in Table 1 with the lifetimes obtained for the conductivity decay in acidic solution. Missing from the table is Cr(sen)$^{3+}$ as its doublet lifetime is too short to be measured. The lifetimes found for *trans*- and *cis*-Cr$(tn)_2(NH_3)_2^{3+}$ agree reasonably well with the data obtained in an earlier study [40] but an error was made in tabulating the values in the thesis [40] and resulting paper [33]. The correct, not the published, lifetimes from that work have been quoted in Table 1. There is reasonably good agreement between the conductivity decay lifetime at pH 3.0 and the emission decay lifetimes for most systems. The somewhat shorter conductivity lifetimes are consistent with the higher temperature at which they were measured. The table shows that *cis*-Cr(cyclam)$(NH_3)_2^{3+}$ is the only complex studied for which the low-pH conductivity lifetime is significantly longer than the emission lifetime.

Table 1
Conductivity and emission decay lifetimes of the Cr(III) complexes

	Conductivity decay lifetime at 22°C (μs)[a]	Doublet emission lifetime at 20°C (μs)	Literature doublet lifetime (μs)	Ref.
$Cr(NH_3)_6^{3+}$	$2.08 \pm 0.06(4)$	$2.39 \pm 0.06(5)$	2.2	[49]
$Cr(en)_3^{3+}$	$1.613 \pm 0.008(4)$	$1.805 \pm 0.016(5)$	1.85	[49]
$Cr(tn)_3^{3+}$	$1.48 \pm 0.17(4)$	$2.04 \pm 0.10(5)$	1.6	[44]
t-$Cr(tn)_2(NH_3)_2^{3+}$	$3.86 \pm 0.17(4)$	$4.58 \pm 0.19(5)$	4.6	[40]
c-$Cr(tn)_2(NH_3)_2^{3+}$	$2.70 \pm 0.08(4)$	$3.36 \pm 0.08(5)$	3.3	[40]
c-Cr(cyclam)$(NH_3)_2^{3+}$	$3.96 \pm 0.11(4)$	$1.66 \pm 0.04(3)$	1.6	[14]

[a] At pH < 3.0. The figure in brackets is the number of measurements.

3.2. pH Dependent conductivity changes

Studies of the pH dependence of the conductivity behavior showed that the complexes fell into two classes, those that gave a monotonic decrease in conductivity throughout the pH range 2.6–5.1 and those that, as the pH was raised, showed evidence for a transient increase followed by a decay. Typical behavior is illustrated in Fig. 3 for $Cr(NH_3)_6^{3+}$ representative of the first type and in Fig. 4 for $Cr(en)_3^{3+}$ representative of the second. Table 2 summarizes the behavior of the complete set of complexes studied. The results obtained for *cis*-Cr(cyclam)$(NH_3)_2^{3+}$ were in good agreement with those reported earlier and we were encouraged that this, along with the lifetime data, confirmed the satisfactory operation of our equipment. Fig. 5 shows some of the data obtained here for *cis*-Cr(cyclam)$(NH_3)_2^{3+}$ as a function of

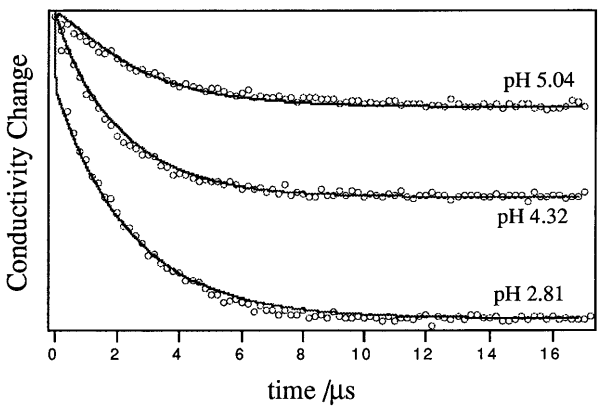

Fig. 3. Conductivity decay curves at various pH for $Cr(NH_3)_6^{3+}$. Legend: (○), experimental points; (—), fit from kinetic modeling.

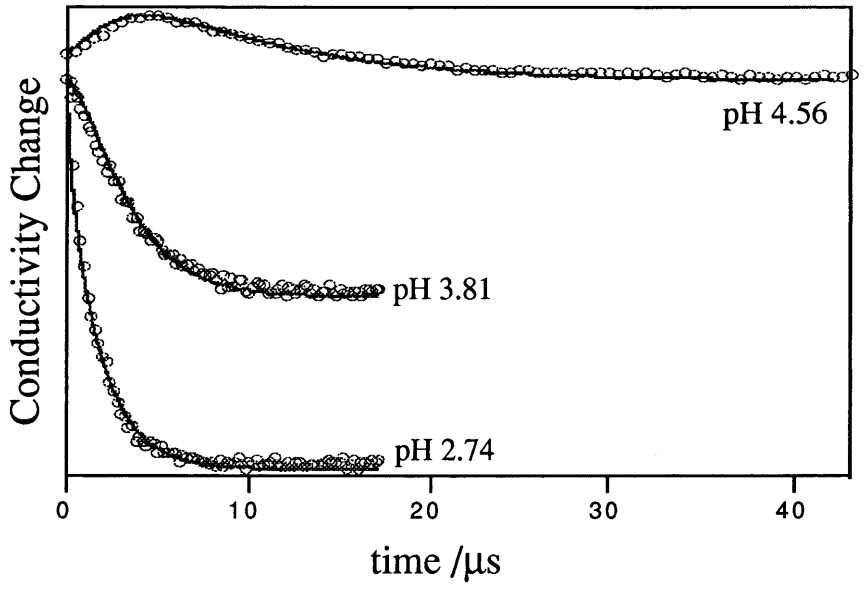

Fig. 4. Conductivity decay curves at various pH for $Cr(en)_3^{3+}$. Legend: (○), experimental points; (—), fit from kinetic modeling.

Table 2
Time-dependent conductivity behavior for the Cr(III) complexes

Complex	$\tau_{cond} > \tau_{emiss}$ at pH < 3	Transient conductivity increases	Dominant photoaquation
cis-$Cr(cyclam)(NH_3)_2^{3+}$	Yes	Yes, pH > 4	NH_3
$Cr(NH_3)_6^{3+}$	No	No	NH_3
cis-$Cr(tn)_2(NH_3)_2^{3+}$	No	No	NH_3
trans-$Cr(tn)_2(NH_3)_2^{3+}$	No	No	NH_3
$Cr(en)_3^{3+}$	No	Yes, pH > 4	en
$Cr(tn)_3^{3+}$	No	Yes, pH > 4	tn
$Cr(sen)^{3+}$	[a]	Yes, pH > 3.5	sen

[a] Observed decay is protonation limited due to fast doublet decay.

pH; there is one new observation not reported earlier, namely that we found a strange kink early in the decay curve at pH 3.85, shown in detail in the inset of Fig. 5. At first we were inclined to dismiss this as an artifact, but the effect was completely reproducible and was seen only for this complex near this pH. As will be discussed later, it turns out to be significant.

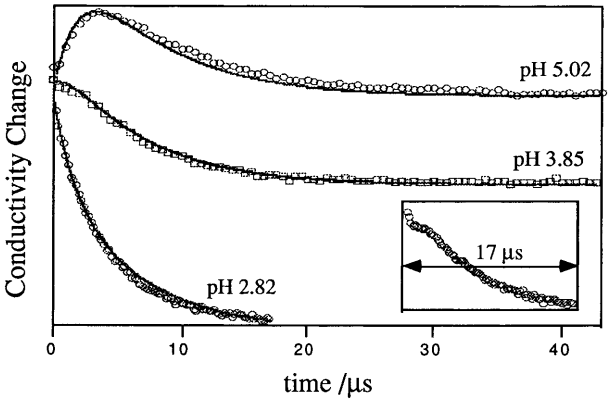

Fig. 5. Conductivity decay curves at various pH for *cis*-Cr(cyclam)$(NH_3)_2^{3+}$. Legend: (○), experimental points; (—), fit from kinetic modeling. The inset shows the first 17 μs of the pH 3.85 trace at higher time resolution.

4. Discussion

4.1. Overview

The summary of the behavior of the systems studied in Table 1 shows that with the exception of *cis*-Cr(cyclam)$(NH_3)_2^{3+}$, all the complexes that lose ammonia as the dominant photoaquation mode give a single exponential decay at all pH values and that at low pH, the lifetime of this conductivity change is the same, within 20%, as the doublet emission decay lifetime. In contrast, the complexes that photoaquate to a product with a monodentate amine arm show a pH-dependent behavior so that at higher pH the time dependence of the conductivity change becomes biexponential.

The complex *cis*-Cr(cyclam)$(NH_3)_2^{3+}$ is in a class of its own because it shows this bimodal pH-dependent conductivity decay at high pH and its single exponential conductivity decay lifetime at pH 3 or below is 4.0 μs (3.7 μs) [14], considerably longer than the emission decay lifetime of 1.6 μs. As Waltz and co-workers have concluded, there is clearly a short-lived (microsecond) aquo-intermediate in this system; we were interested in whether such intermediates were present in any of the other systems and if not, why not? Clearly in none of the other systems is there an intermediate of lifetime longer than the doublet lifetime, but there are systems that show pH-dependent bimodal conductivity decay curves. To explore the significance of these observations, we have compared the conductivity behavior to calculations of the conductivity changes expected based on integration of the complete kinetic equations for the photoaquation process for each complex studied. Naturally we began with the $Cr(NH_3)_6^{3+}$ system as its photochemistry is well understood and it represents a useful starting point and an important test of the feasibility of the calculations.

4.2. Data modeling for $Cr(NH_3)_6^{3+}$

This compound is known to photoaquate in 74% yield via the doublet and 26% via the quartet state [44], and the overall quantum yield of photoaquation [7] is 0.44. Under our conditions, the doublet lifetime is 2.4 μs. The photoproduct is $Cr(NH_3)_5H_2O^{3+}$ which undergoes an acid/base dissociation with a pK_a of between 5.1 and 5.3 [46]. Free ammonia arising from the photoaquation is protonated with a rate constant [47] of 4.3×10^{10} M^{-1} s^{-1}. Using this information and estimated molar conductivity values for the complexes, the time dependence of the conductivity change was modeled for the mechanism (Scheme 1):

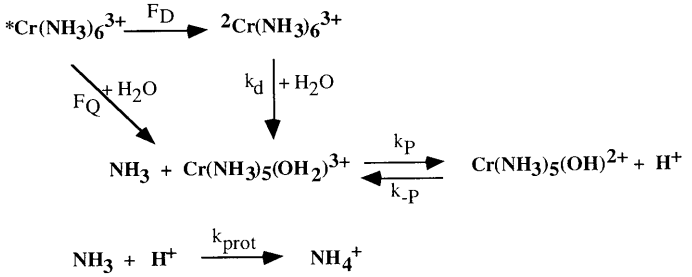

Scheme 1.

In this and subsequent schemes, deactivation of excited state Cr(III) species to the ground state has been omitted for simplicity; F_Q and F_D are the fractions of reaction that occur via quartet and doublet states, respectively. Fig. 3 shows that it is possible to fit the data from pH 2.8 to 5.04 with a single set of rate constants and conductivities, using experimental values for known quantities, and reasonable estimates for those not available. The good agreement between experimental and modeled data supports the validity of modeling.

The results confirm that at low pH there is a prompt conductivity decrease corresponding to about 25% of the reaction, followed by a single exponential conductivity decrease with the doublet lifetime. It can be seen in Fig. 3 that the prompt component occurs faster than the experimental change, but this is merely because the apparatus response is too slow ($\tau \approx 50$ ns) to follow the very rapid protonation of released ammonia. At higher pH values, the prompt decrease is no longer seen; this is because at these lower proton concentrations, protonation of the ammonia liberated in the prompt photoaquation has become slower and is occurring on a similar time-scale to that of the photoaquation mediated by the doublet state. For the same reasons, at higher pH values the conductivity decay becomes somewhat nonexponential with a lifetime longer than the doublet lifetime; we have confirmed that the latter is independent of pH, as monitored by the emission decay. The extent of the overall conductivity decay decreases at higher pH owing to the acid–base equilibrium of the aquo-product.

Analogous behavior was observed for *trans*- and *cis*-$Cr(tn)_2(NH_3)_2^{3+}$, and the data over the whole pH range was again successfully modeled using reasonable rate

constant and conductivity values along with 15% prompt and 85% slow reaction. The small yield, $< 10\%$, of 1,3-propanediamine photoaquation in this system was ignored in the modeling.

4.3. Data modeling for $Cr(en)_3^{3+}$

The data for the systems which photoaquate one end of a bidentate ligand, and which also undergo both prompt and slow photoprocesses require an additional step in the mechanism. For example, for $Cr(en)_3^{3+}$ the initial photoproduct formed is expected to be an aquo-substituted species with a monodentate free amine ligand, $Cr(en)_2(en\text{–})(OH_2)^{3+}$. This species can participate in two different acid–base reactions before finally achieving the final product equilibrium position, loss of proton from the coordinated water ligand and protonation of the free amine moiety. It is the competition between these processes that dictates the conductivity behavior. The complete mechanistic scheme can be written (Scheme 2):

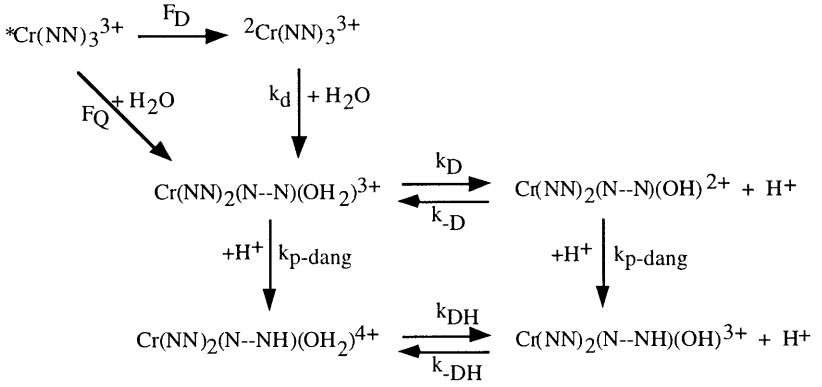

Scheme 2.

Fig. 4 shows the comparison of the modeled data at pH 3.81 and the extremes of 2.74 and 4.56, where again a single set of parameters has been used to fit the data throughout the pH range. These parameters included the literature values for the pK_a [48] of $Cr(en)_2(enH)(H_2O)^{4+}$ and for the protonation rate constant [42] for $Cr(en)_2(en\text{–})(H_2O)^{3+}$ of 3.6×10^9 M^{-1} s^{-1}, significantly smaller than the rate constant for ammonia protonation. The agreement is satisfactory although not perfect, but gives us some confidence in the basic correctness of the mechanism. The important feature of this modeling is that, because of the lower protonation rate constant for the monodentate ethylenediamine ligand, there is the opportunity for the primary product, the six-coordinate aquo-complex $Cr(en)_2(en\text{–})(OH_2)^{3+}$, to deprotonate in competition with protonation of the released amine N, thus giving rise to proton release and a conductivity increase. Consequently at higher pH, the primary product of the photochemistry is not in acid–base equilibrium and should therefore strictly be considered an 'intermediate'. In this respect, the pH-dependent conductivity behavior mimics that of *cis*-$Cr(cyclam)(NH_3)_2^{3+}$.

The complex $Cr(tn)_3^{3+}$ can be modeled in a similar way to that outlined here for $Cr(en)_3^{3+}$. $Cr(sen)^{3+}$ behaves and can be modeled similarly, but it has a doublet state lifetime less than 5 ns so that rate constants other than that for doublet decay determine the time-dependent behavior. Also we find it gives several photoproducts and the study of this complex has not yet been finalized.

4.4. The intermediate and data modeling for *cis*-$Cr(cyclam)(NH_3)_2^{3+}$

The biexponential conductivity behavior displayed by *cis*-$Cr(cyclam)(NH_3)_2^{3+}$ is similar to that observed for the complexes which photoaquate to give a dangling amine arm, yet the only observed photoproduct, *cis*-$Cr(cyclam)(NH_3)(OH_2)^{3+}$, indicates loss of an ammonia ligand. Clearly the intermediate occurring in the photolysis of this complex differs from those found for $Cr(en)_3^{3+}$, $Cr(tn)_3^{3+}$ and $Cr(sen)^{3+}$. The question becomes, why is the behavior of *cis*-$Cr(cyclam)(NH_3)_2^{3+}$ unique?

In the introduction and Fig. 2 we presented the literature mechanism for the photochemistry of *cis*-$Cr(cyclam)(NH_3)_2^{3+}$. Naturally, in our initial modeling we attempted to fit our observed pH-dependent conductivity changes to this mechanism. To our surprise, the scheme failed to provide a set of parameters capable of fitting the conductivity changes throughout the pH range 2.82–5.02 so it was necessary to modify it. In the first instance, we found it necessary to incorporate two reaction modes, first direct loss of ammonia and a second mode that gave rise to the long lived intermediate. This intermediate has the characteristics that it gives rise eventually to the same products as the direct ammonia loss mode. Friesen et al. considered two possibilities for this species; a seven coordinate aquo complex, or a six-coordinate complex in which one cyclam ring N has been dissociated.

We prefer this last choice for theoretical reasons. First, were it to be a genuine seven-coordinate species, why is it unique to this complex and why did we not find similar behavior in any of the other complexes we have examined? Note here that although seven-coordinate intermediates have also been proposed [25] for the polypyridyl complexes, the intermediates have been suggested [45] to be six-coordinate in more recent work. Secondly the angular overlap model provides a nice rationale for this unique behavior of *cis*-$Cr(cyclam)(NH_3)_2^{3+}$. As a first approximation, ignore the slightly different ligand field strengths of cyclam-N and ammonia.

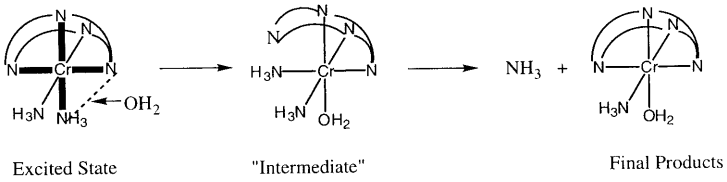

Fig. 6. Proposed mechanism for cyclam ring-N labilization and recombination with ammonia loss. The heavy bonds indicate the plane of excitation, and the edge-displacement process should be confined to this plane.

Fig. 6 shows excitation in one of the three orthogonal planes corresponding to one component of the $^4T_{2g}$ excited state. This labilizes an ammonia ligand, implying the possibility of direct ammonia labilization to final products, and also labilizes three of the cyclam-N ligands. (If the greater ligand field strength of cyclam-N is recognized, the AOM model and Adamson's rule both predict preferential labilization of cyclam nitrogen.) If a cyclam-N can be displaced as shown in Fig. 6, then the stereochemical change feature of Cr(III) photochemistry implies that the ammonia ligand will migrate to occupy the vacated ligand site as shown. This gives a six-coordinate aquo-intermediate that, when the ring-N re-coordinates, will expel the ammonia ligand to give the same final products as were obtained by direct ammonia loss. This is exactly the behavior required by the experimental observations. We have therefore incorporated this type of intermediate into the modeling of the photoaquation of *cis*-Cr(cyclam)$(NH_3)_2^{3+}$.

Scheme 3 shows the kinetic model used. It has been simplified by not showing the individual prompt and slow components of the reaction, but as for the other systems, the complete modeling includes the parameter F_D and assumes that the photoproducts obtained via the quartet and doublet routes are identical. The best modeling of the experimental data was obtained for $F_D = 0.70$, a value typical of the experimental values for other hexam(m)ine complexes. Details of the equations used, initial conditions and derived parameters are given in Appendix A.

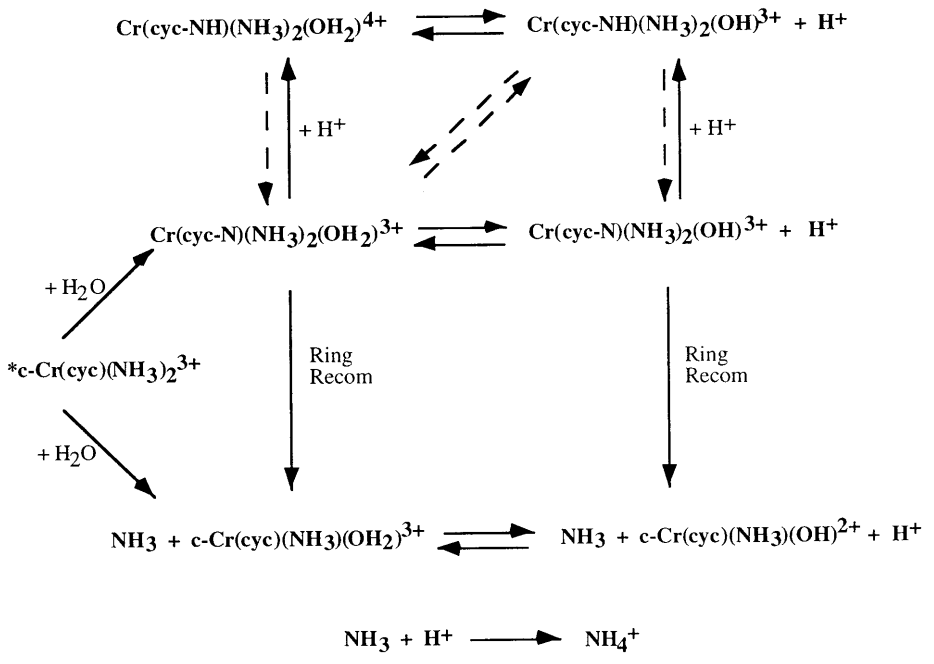

Scheme 3.

With this scheme we were able to fit the conductivity decay data throughout the pH range, including the 'kink' observed at pH 3.85, with a single set of parameters. Representative fits are shown in Fig. 5. The best fits to the experimental data were obtained with the cyclam loss mode dominating, accounting for 67% of the overall photochemistry. The unique conductivity behavior exhibited by *cis*-Cr(cyclam)$(NH_3)_2^{3+}$ results from the photochemistry occurring via the cyclam ring-N mode.

The conductivity decay lifetime observed at pH 3 is a composite of the cyclam ring-N and direct ammonia loss modes. The best fits gave recombination rate constants, k_{rec} and $k_{rec'}$, for the labilized cyclam-N of 2.4×10^5 and 1.4×10^5 s^{-1}, respectively, both significantly smaller than the doublet emission decay rate constant of 6.25×10^5 s^{-1} and therefore rate-determining for the ammonia release and subsequent protonation via ring-N recombination. Because of this, the observed conductivity decay lifetime in acid solution is significantly longer than the doublet lifetime. In addition, the slow recombination rate of the cyclam-N causes delayed ammonia release and protonation, giving time for deprotonation of the aquo-intermediate at higher pH values; this results in the transient increases in solution conductivity.

For this system, Friesen et al. [14] concluded that less than 10% of the reaction could be prompt. In the successful modeling discussed above, 30% of the photochemistry occurs via the prompt route; however, the fraction of the proton uptake that results via cyclam-N loss and ammonia release is rate-limited by the slow recombination step and is therefore not observed on the prompt time scale. Only the prompt 30% of the 33% of photoreaction that releases ammonia directly can be seen as a prompt conductivity decrease, i.e. about 10% of the overall conductivity decrease. This is in excellent agreement with the 10% prompt decay that we also estimate by analyzing the data at low pH using a simple two-component exponential decay. Also it is this 10% of observable prompt photoreaction that generates the kink seen in the conductivity traces at pH 3.85 (Fig. 5).

4.5. Conclusions and on-going work

In this work, intermediates have been observed in the photoaquation reactions of complexes with bidentate or multidentate ligands, but generally they are rather mundane in nature, being primary photoproducts susceptible to rapid acid/base equilibration of coordinated water and free amine ligand. The exception to date is *cis*-Cr(cyclam)$(NH_3)_2^{3+}$, which forms an intermediate with a microsecond lifetime longer than that of its doublet state.

In the literature this intermediate has been proposed to be seven-coordinate and has been cited as supporting a pathway of doublet decay via vibrationally-promoted crossing to an electronically ground state intermediate. The present work suggests rather that the intermediate is a conventional six-coordinate photoproduct with an uncoordinated cyclam ring-N; this primary photoproduct is metastable and the cyclam ligand re-coordinates to displace ammonia and produce the stable final products. It is therefore likely that the intermediate does not have the mechanistic significance that has been attributed [35] to it. Our efforts to identify or trap an intermediate of this type have so far been unsuccessful, but efforts to do so are continuing.

Acknowledgements

The authors thank the Natural Sciences and Engineering Research Council and the University of Victoria for financial support of this work. We thank Dr W. Waltz for helpful discussions and for providing pre-publication copies of his work. ADK wishes to thank Arthur Adamson for stimulating discussions and advice.

Appendix A. Equations, initial conditions and derived parameters for *cis*-$Cr(cyclam)(NH_3)_2^{3+}$

Symbols

$^{D}Cr = Cr(cyc)(NH_3)_2^{3+}$ doublet state
$P\_OH_2 = Cr(cyc)(NH_3)(OH_2)^{3+}$
$I\_OH_2 = Cr(cyc\text{-}N)(NH_3)_2(OH_2)^{3+}$
$IH\_OH_2 = Cr(cyc\text{-}NH)(NH_3)_2(OH_2)^{4+}$
λ_{4+} = molar conductivity of Cr^{4+} species
λ_{2+} = molar conductivity of Cr^{2+} species
$P\_OH = Cr(cyc)(NH_3)(OH)^{2+}$
$I\_OH = Cr(cyc\text{-}N)(NH_3)_2(OH)^{2+}$
$IH\_OH = Cr(cyc\text{-}NH)(NH_3)_2(OH)^{3+}$
λ_{3+} = molar conductivity of Cr^{3+} species
For other symbols see Scheme 3

Differential rate equations

$$d[^{D}Cr]/dt = -k_{D}*[^{D}Cr]$$

$$d[H^+]/dt = k_I*[I\_OH_2] - k_{\_I}*[I\_OH]*[H^+] + k_{IH}*[IH\_OH_2] - k_{\_IH}*[IH\_OH]*[H^+] - k\,p_{cycN}*[I\_OH_2]*[H^+] - k\,p_{cycN}*[I\_OH]*[H^+] - k_{\_P}*[P-OH]*[H^+] + k_P*[P-OH_2] - k_{prot}*[NH_3]*[H^+]$$

$$d[I\_OH_2]/dt = Ø*F_{cyc}*k_D*[^{D}Cr] + k_{\_I}*[I\_OH]*[H^+] - k\,p_{cycN}*[I\_OH_2]*[H^+] - k_I*[I\_OH_2] - k_{rec}*[I\_OH_2] + k_I*[IH\_OH]$$

$$d[IH\_OH_2]/dt = k\,p_{cycN}*[I\_OH_2]*[H^+] + k_{\_IH}*[IH\_OH]*[H^+] - k_{IH}*[IH\_OH_2]$$

$$d[I\_OH]/dt = k_I*[I\_OH_2] - k_{\_I}*[I\_OH]*[H^+] - k_{pcycN}*[I\_OH]*[H^+] - k_{rec'}*[I\_OH]$$

$$d[IH\_OH]/dt = k_{IH}*[IH\_OH_2] + k_{pcycN}*[I\_OH]*[H^+] - k_{\_IH}*[IH\_OH]*[H^+] - k_I*[IH\_OH]$$

$$d[P-OH_2]/dt = Ø*(1-F_{cyc})*k_d*comp + k_{\_P}*[P-OH]*[H^+] - k_P*[P-OH_2] + k_{rec}*[I\_OH_2]$$

$$d[P-OH]/dt = k_P*[P-OH_2] - k_{\_P}*[P-OH]*[H^+] + k_{rec'}*[I\_OH])$$

$$d[NH_3]/dt = Ø*(1-F_{cyc})*k_D*[^DCr] - k_{prot}*[NH_3]*[H^+] + k_{rec}*([I\_OH_2] + k_{rec'}*[I\_OH]$$

$$d[NH_4^+]/dt = k_{prot}*[NH_3]*[H^+]$$

Calculation of time dependent conductivity changes

$$H_t = [H^+]_t - [H^+]_{t=0}$$

$$K_t = \lambda_{H+}*H_t + (\lambda_{4+} - \lambda_{3+})*[IH\_OH_2]_t - (\lambda_{3+} - \lambda_{2+})*[I\_OH]_t + \lambda_{NH_{4+}}*[NH_4]_t - (\lambda_{3+} - \lambda_{2+})*[P-OH]_t$$

Initial conditions

$$[^DCr]_{t=0} = I_a \cdot F_D;\ [IH\_OH_2]_{t=0} = I_a \cdot F_Q \cdot F_{cyc;}\ [P-OH_2]_{t=0} = [NH_3]_{t=0} = I_a \cdot F_Q \cdot (1-F_{cyc})$$

Table of fit parameters

Variable	Modeled value	Variable	Modeled value
F_D	0.70	pK_P	4.2
$Φ$	0.10[a]	$k_{\_P}$ (M^{-1} s^{-1})	7.0×10^9
F_{cyc}	0.67	k_P (s^{-1})	4.4×10^{5}[d]
ε_{355} (M^{-1} cm^{-1})	90[a]	pK_I	4.1
k_d (s^{-1})	6.25×10^{5}[a]	$k_{\_I}$ (M^{-1} s^{-1})	6.0×10^9
k_{p-cycN} (M^{-1} s^{-1})	8×10^7	k_I (s^{-1})	9.5×10^{5}[d]
k_{prot} (M^{-1} s^{-1})	4.3×10^{10}[a]	pK_{IH}	3.8
$\lambda_{3+}\times10^{-4}$ (S m^2 mol^{-1})	174[a]	$k_{\_IH}$ (M^{-1} s^{-1})	4.0×10^9
$\lambda_{2+}\times10^{-4}$ (S m^2 mol^{-1})	116[b]	k_{IH} (s^{-1})	3.2×10^{5}[d]
$\lambda_{4+}\times10^{-4}$ (S m^2 mol^{-1})	232[b]	k_{rec} (s^{-1})	2.35×10^5
k_{int} (s^{-1})	5.0×10^{8}[c]	$k_{rec'}$ (s^{-1})	1.35×10^5

[a]Measured k_{prot} from Ref. [47].
[b]Estimated based on λ^{3+} value and charge ratio.
[c]It is likely that k_{int} is much larger than this given value, but the delta time of the modeling is too large to permit use of a greater value. This does not affect the modeled results.
[d]Not an independent variable; listed for the convenience of the reader.

References

[1] A.W. Adamson, J. Phys. Chem. 71 (1967) 798.
[2] P. Riccieri, E. Zinato, J. Am. Chem. Soc. 97 (1975) 6071.
[3] A.D. Kirk, Coord. Chem. Rev. 39 (1981) 225.
[4] C. Kutal, A.W. Adamson, J. Am. Chem. Soc. 93 (1971) 5581.
[5] C. Kutal, A.W. Adamson, Inorg. Chem. 12 (1973) 1990.
[6] L.G. Vanquickenborne, A. Ceulemans, Coord. Chem. Rev. 48 (1983) 157.
[7] A.D. Kirk, Chem. Rev. 99 (1999) 1607.
[8] L.G. Vanquickenborne, A. Ceulemans, J. Am. Chem. Soc. 99 (1977) 2208.
[9] L.G. Vanquickenborne, A. Ceulemans, J. Am. Chem. Soc. 100 (1978) 475.
[10] S.T.J. Spees, J.R. Perumareddi, A.W. Adamson, J. Am. Chem. Soc. 90 (1968) 6626.
[11] K. Angermann, R. Van Eldik, H. Kelm, F. Wasgestian, Inorg. Chim. Acta 49 (1981) 247.
[12] K. Angermann, R. Van Eldik, H. Kelm, F. Wasgestian, Inorg. Chem. 20 (1981) 955.
[13] K. Angermann, R. Schmidt, R. Van Eldik, H. Kelm, F. Wasgestian, Inorg. Chem. 21 (1982) 1175.
[14] D.A. Friesen, S.H. Lee, J. Lilie, W.L. Waltz, L. Vincze, Inorg. Chem. 30 (1991) 1975.
[15] D.A. Friesen, S.H. Lee, R.E. Nashiem, S.P. Mezyk, W.L. Waltz, Inorg. Chem. 34 (1995) 4026.
[16] L. Vincze, D.A. Friesen, S.P. Mezyk, W.L. Waltz, Inorg. Chem. 31 (1992) 4950.
[17] A.D. Kirk, Comments Inorg. Chem. 14 (1993) 89.
[18] L. Moensted, O. Moensted, Coord. Chem. Rev. 94 (1989) 109.
[19] H.H. Krause, F. Wasgestian, Inorg. Chim. Acta 29 (1978) 231.
[20] J.F. Endicott, Comments Inorg. Chem. 3 (1985) 349.
[21] L.G. Vanquickenborne, A. Ceulemans, Inorg. Chem. 20 (1981) 110.
[22] G. Neshvad, M.Z. Hoffman, M. Bolte, R. Sriram, N. Serpone, Inorg. Chem. 26 (1987) 2984.
[23] M.A. Jamieson, N. Serpone, M. Maestri, Inorg. Chem. 17 (1978) 2432.
[24] M.A. Jamieson, N. Serpone, M.Z. Hoffman, J. Am. Chem. Soc. 105 (1983) 2933.
[25] F. Bolletta, M. Maestri, L. Moggi, M.A. Jamieson, N. Serpone, M.S. Henry, M.Z. Hoffman, Inorg. Chem. 22 (1983) 2502.
[26] R. Fukuda, R.T. Walters, H. Macke, A.W. Adamson, J. Phys. Chem. 83 (1979) 2097.
[27] A.D. Kirk, P.E. Hoggard, G.B. Porter, M.G. Rockley, M.W. Windsor, Chem. Phys. Lett. 37 (1976) 199.
[28] P.E. Hoggard, A.D. Kirk, G.B. Porter, M.G. Rockley, M.W. Windsor, NBS Spec. Publ. 526 (1978) 137.
[29] G.E. Rojas, C. Dupuy, D.A. Sexton, D. Magde, J. Phys. Chem. 90 (1986) 87.
[30] G.E. Rojas, D. Magde, J. Phys. Chem. 91 (1987) 689.
[31] W.L. Waltz, S.H. Lee, D.A. Friesen, J. Lilie, Inorg. Chem. 27 (1988) 1132.
[32] A.D. Kirk, M.A.R. Scandola, J. Phys. Chem. 86 (1982) 4141.
[33] A.D. Kirk, A.M. Ibrahim, Inorg. Chem. 27 (1988) 4567.
[34] I. Mackay, Ph.D. Dissertation, University of Victoria, 1998.
[35] M.W. Perkovic, M.J. Heeg, J.F. Endicott, Inorg. Chem. 30 (1991) 3140.
[36] A.L. Oppegard, J.C.J. Bailar, Inorg. Synth. 3 (1950) 153.
[37] J. Ferguson, M.L. Tobe, Inorg. Chim. Acta 4 (1970) 109.
[38] S.R.L. Fernando, Ph.D. Dissertation, University of Victoria, 1994.
[39] J.W. Vaughn, O.J. Stvan, V.E. Magnuson, Inorg. Chem. 7 (1968) 736.
[40] M.I. Ibrahim, Ph.D. Dissertation, University of Victoria, 1989.
[41] G. Irwin, Ph.D. Dissertation, University of Victoria, 1999.
[42] W.L. Waltz, R.T. Walters, R.J. Woods, J. Lilie, Inorg. Chim. Acta 45 (1980) L153.
[43] J. Lilie, W.L. Waltz, Inorg. Chem. 22 (1983) 1473.
[44] W.L. Waltz, J. Lilie, S.H. Lee, Inorg. Chem. 23 (1984) 1768.
[45] J. Lilie, W.L. Waltz, S.H. Lee, L.L. Gregor, Inorg. Chem. 25 (1986) 4487.
[46] C.S. Garner, D.A. House, in: R.L. Carlin (Ed.), Transition Metal Chemistry, vol. 6, Marcel Dekker, New York, 1970.
[47] M. Eigen, Angew. Chem. 75 (1963) 489.
[48] P. Andersen, T. Berg, J. Jacobsen, Acta Chem. Scand. A 29 (1975) 381.
[49] R.T. Walters, A.W. Adamson, Acta Chem. Scand. A 33 (1979) 53.